

RESEARCH ARTICLE | AUGUST 15 2024

# Observation of enhanced heat transfer between a nanotip and substrate at nanoscale distances via direct temperature probing with Raman spectroscopy

Xiaona Huang ; Qiangsheng Sun; Shen Xu ; Yanan Yue  ; Xinwei Wang ; Yimin Xuan 

 Check for updates

*Appl. Phys. Lett.* 125, 072201 (2024)

<https://doi.org/10.1063/5.0222178>



15 August 2024 14:20:01

Nanotechnology & Materials Science


Optics & Photonics

Impedance Analysis

Scanning Probe Microscopy


Sensors

Failure Analysis & Semiconductors



**Unlock the Full Spectrum.**  
From DC to 8.5 GHz.  
Your Application. Measured.

[Find out more](#)



# Observation of enhanced heat transfer between a nanotip and substrate at nanoscale distances via direct temperature probing with Raman spectroscopy

Cite as: Appl. Phys. Lett. **125**, 072201 (2024); doi: [10.1063/5.0222178](https://doi.org/10.1063/5.0222178)

Submitted: 6 June 2024 · Accepted: 3 August 2024 ·

Published Online: 15 August 2024








View Online



Export Citation



CrossMark

Xiaona Huang,<sup>1</sup>  Qiangsheng Sun,<sup>1</sup> Shen Xu,<sup>2</sup>  Yanan Yue,<sup>1,3,a)</sup>  Xinwei Wang,<sup>4</sup>  and Yimin Xuan<sup>5</sup> 

## AFFILIATIONS

<sup>1</sup>School of Power and Mechanical Engineering, Wuhan University, Wuhan, Hubei 430072, China

<sup>2</sup>School of Mechanical and Automotive Engineering, Shanghai University of Engineering Science, Shanghai 201620, China

<sup>3</sup>Department of Mechanical and Manufacturing Engineering, Miami University, Oxford, Ohio 45056, USA

<sup>4</sup>Department of Mechanical Engineering, Iowa State University, Ames, Iowa 50011, USA

<sup>5</sup>School of Energy and Power Engineering, Nanjing University of Aeronautics and Astronautics, Nanjing 210016, China

<sup>a)</sup> Author to whom correspondence should be addressed: [yyue@whu.edu.cn](mailto:yyue@whu.edu.cn)

## ABSTRACT

Nanoscale heat transfer between two nanostructured surfaces holds paramount significance in the realms of extreme manufacturing and high-density data storage. However, experimental probing of heat transfer encounters significant challenges, primarily due to limitations in current instrumentation. Here, we report a method based on Raman spectroscopy to directly probe the temperature difference between a Si nanotip and SiC substrate. Results indicate a decrease in substrate temperature, while the temperature of the nanotip remains relatively stable as the nanotip moves away from the substrate from approximately 82.5 to 1320 nm. We trace this enhanced heat transfer to a significant augmentation, by one order of magnitude, in air conduction and thermal radiation energy exchange theoretically, with air conduction being the dominant mode over thermal radiation. This work advances the direct observation of surface temperatures with gaps smaller than 1  $\mu\text{m}$ , utilizing a noncontact and nondestructive Raman technique, which can be extended to studying near-field heat transfer across various Raman-active surfaces.

Published under an exclusive license by AIP Publishing. <https://doi.org/10.1063/5.0222178>

Heat transfer between surfaces separated by sub-micro distances has triggered broad interest due to the fast development in the fields of thermal management,<sup>1</sup> energy conversion,<sup>2</sup> and data storage.<sup>3</sup> At such small scales, air conduction and radiation heat transfer exhibit behaviors distinct from macro-scale processes. Air conduction shows diffusive, transition, and ballistic regime characteristics as the distance decreases from the microscale to the nanoscale.<sup>4</sup> Moreover, radiation heat transfer can increase by orders of magnitude and greatly surpass Planck's blackbody limit in the near field (sub-wavelength gap distance) due to the tunneling of evanescent modes.<sup>5</sup> Despite the fast theoretical development of these intriguing phenomena,<sup>5</sup> experimental studies at such small scales have persistently posed challenges due to the constraints associated with prevailing measurement methods on accurate control of distance and precise measurement of temperature and power.

Nevertheless, numerous endeavors have been undertaken to quantify near-field heat transfer, with a particular emphasis on radiation heat transfer, where temperature determination plays a pivotal role. Scanning thermal microscopy (SThM) probe, functioning both as a heater and a thermistor, enables the measurement of thermal conductivity in thin films.<sup>7,8</sup> And Reddy's group successfully measured the near-field radiation by integrating an SThM probe with an embedded thermocouple to probe temperature.<sup>9</sup> In addition, radiation enhancement in the near-field regime between two parallel plates has been studied with embedded temperature sensors on/near surfaces.<sup>10–12</sup> These methodologies push forward the near-field heat transfer studies, while it is a struggle to directly measure the temperatures of both heat exchange surfaces. The techniques predominantly rely on single-sided measurements or derive temperatures from thermal resistance and near-surface measurements. To date, there has been an absence of

efforts toward establishing a direct, double-sided temperature measurement approach, which is crucial for a comprehensive understanding of near-field heat transfer in practice.

Raman spectroscopy as a noncontact measurement provides easy access to micro/nanoscale environments.<sup>13–15</sup> It has been used to investigate the thermal transport in suspended single-layer graphene in early studies.<sup>16,17</sup> Recently, Shi *et al.* distinguished the effects of hot phonons and thermal stress in micro-Raman spectra of MoS<sub>2</sub>.<sup>18</sup> Moreover, tip-enhanced Raman spectroscopy enabled temperature measurement within a sub-10 nm laser-induced hot spot in GaN, facilitating experimental analysis of associated ballistic thermal transport processes.<sup>19</sup> Therefore, Raman spectroscopy measurement emerges as a promising method for non-invasively directly measuring the temperatures of two heat exchange surfaces without causing structural damage. Here, we focus on the heat transfer between a nanotip and substrate, which is crucial for extreme manufacturing<sup>20</sup> and high-density data storage<sup>21</sup> realms. Raman thermal measurement system and atomic force microscopy (AFM) are combined, which facilitates precise control over the nanotip–substrate gap size and simultaneous characterization of their temperatures. Significantly enhanced heat transfer is observed as the gap size decreases from approximately 1.32  $\mu\text{m}$  to about 82.5 nm, which is further corroborated by theoretical calculations.

A key challenge in conducting near-field heat transfer experiments lies in the stable control of the gap between two surfaces at a sub-wavelength scale. We employ AFM and Raman spectrometer to study the near-field heat transfer between two surfaces with gap distances as small as tens of nanometers [see Fig. 1(a)]. Our designed setup utilizes a small-angle aligned laser with the substrate to heat the nanotip and excite the Raman signal of the substrate, rather than generating a tip-enhanced optical field. Optical lever detection is used to

accurately determine the position of the nanotip by analyzing the reflected laser beam off the back of the cantilever. Thereafter, a piezoelectric actuator is used to generate precise nanoscale motion of a Si nanotip (BudgetSensors, Tap190Al-G) in response to an applied voltage. The Si nanotip, with a length of 17  $\mu\text{m}$ , features a curvature radius of 10 nm at the apex and a half cone angle of 10° [see Fig. 1(b)]. Regarding the substrate, a bulk 4H-SiC wafer, with dimensions of 10  $\times$  10  $\times$  0.5 mm<sup>3</sup>, is grown by the seed crystal method and has a roughness of less than 0.9 nm after polishing [see Fig. 1(c)]. Simultaneously, the Raman thermal measurement technique is applied to capture Raman scattering from both the tip and the substrate.

A 532 nm continuous wave laser (5.1 mW) is focused onto the nanotip using a 50 $\times$  objective and high precision 3D displacement stage. The laser power is selected to ensure sufficient heat transfer between the tip and the substrate. Reducing the laser power leads to a lower temperature rise at the nanotip and the substrate, resulting in weaker heat exchange between the two surfaces. And lower laser energy yields a weaker Raman signal from the surfaces, which introduces additional challenges in spectroscopy measurement and increases the complexity of data processing. The radius of the laser spot at the focal level is around 17.5  $\mu\text{m}$ . Through the same objective, the Raman scattering signal is collected and directed to a spectrometer for subsequent translation of the Raman spectrum, with the gratings of 1800 grooves/mm to enhance Raman resolution. A typical Raman spectrum in this configuration is depicted in Fig. 1(d), exhibiting robust Raman peaks stemming from the E<sub>2</sub>(TO), E<sub>1</sub>(TO), and A<sub>1</sub>(LO) active phonon modes within the SiC substrate,<sup>22</sup> alongside the first-order optical characteristic mode in the Si nanotip.<sup>23</sup> This setup facilitates the simultaneous *in situ* detection of their respective temperatures. The typical peaks from Si and the A<sub>1</sub>(LO) mode from SiC, centered around 520.7 and 964.0 cm<sup>-1</sup> at room temperature, are chosen to quantify

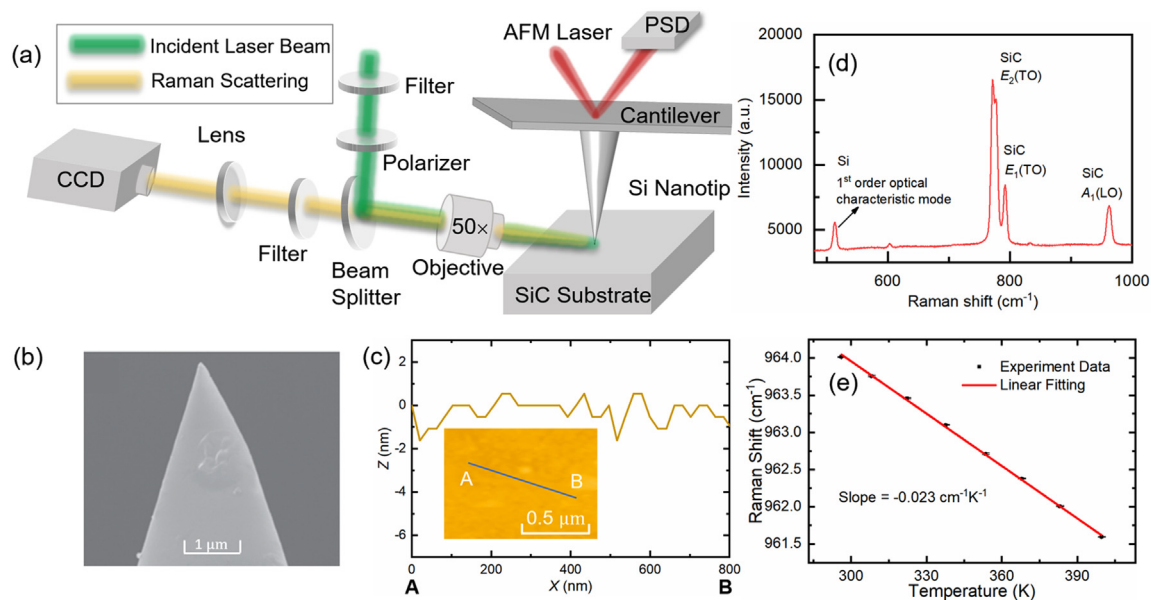


**FIG. 1.** (a) Schematic illustration of the experimental setup. A focused 532 nm laser beam serves to excite Raman scattering signals concurrently from both the nanotip and the substrate. (b) Scanning electron microscopy (SEM) image of the nanotip. (c) Atomic force microscopy (AFM) image of SiC substrate. (d) Raman spectrum of Si nanotip and SiC substrate. (e) Raman shift-temperature calibration results of SiC.

temperature changes due to their distinct peaks and high intensities. The Raman shift of each peak is obtained by fitting the peak using the Lorentz function. Three spectra are collected at each measurement and averaged to reduce measurement uncertainty. An operating period of approximate 30 min is maintained before spectra collection to ensure the attainment of a steady-state thermal transport condition within the tip–substrate system. Our calibration experiments show a good linear relationship between Raman shift and temperature in Si and SiC, demonstrating slopes of  $-0.022$  and  $-0.023 \text{ cm}^{-1} \text{ K}^{-1}$ , respectively [see [supplementary material](#) Note 1 and [Fig. 1\(e\)](#)].

The experiments are carried out under ambient air conditions at room temperature. Initially, the nanotip approaches the substrate until they reach a nearly contacted state. Subsequently, the objective is carefully adjusted to focus the laser spot onto the tip apex. In detail, the objective is adjusted in the plane normal to the tip axis to maximize the intensity of the Si Raman peak, ensuring the laser spot is focused on the tip center. Then, the objective is moved along the tip axis to focus the laser spot on the tip apex through making sure the Raman signal can just be detected. During experiments, the tip is moved away from the substrate in nanoscale steps from the near contact mode along the vertical direction (nanotip axis) using a piezoelectric actuator, with the distance ranging from 82.5 to 1320.0 nm. The nanotip moves around  $1 \mu\text{m}$  during our measurements, which is much smaller than the laser spot. Thus, the radius of the laser spot ensures good coverage of both the nanotip apex and the substrate surface beneath the tip.

During movement of the nanotip away from the substrate, as illustrated in [Figs. 2\(a\) and 2\(b\)](#), the Raman shift of the tip exhibits only marginal variations, whereas the substrate's Raman shift undergoes a significant increase, as depicted in [Figs. 2\(c\)–2\(f\)](#). Based on the linear relationship between the Raman shift and temperature, when the nanotip moves backward, its temperature remains steady at approximately  $200 \text{ }^\circ\text{C}$ , while the temperature of the substrate decreases from about  $32.6$  to  $22.4 \text{ }^\circ\text{C}$  [[Fig. 2\(g\)](#)]. Notably, the incident laser is sharply focused by the nanotip onto the SiC substrate, and the excited Raman scattering of SiC originates from the confined region beneath the tip. This scattering is then reflected by the tip, eventually being collected by the objectives and the CCD. This process is consistent with the observed increase in intensity of Si and SiC peaks as the gap size between the tip and substrate decreases [[Figs. 2\(c\) and 2\(d\)](#)]. Consequently, the Raman signal represents the localized temperature of the confined region. The observed decrease in temperature indicates reduced energy absorption by the substrate as the tip moves away, highlighting a significant enhancement in heat transfer when their distance is reduced to the nanoscale. In addition, the error of temperature measurement in our experiments is determined by the error associated with the Raman shift. The maximum Raman shift errors from fitting for the nanotip and the substrate are  $\pm 0.026$  and  $\pm 0.010 \text{ cm}^{-1}$ , respectively. Thus, their corresponding temperature uncertainties are  $\pm 1.2$  and  $\pm 0.4 \text{ }^\circ\text{C}$ , respectively.

Various factors may contribute to the temperature change in substrate, including laser irradiation, electromagnetic field enhancement due to the tip-enhanced effect, and heat transfer from the hot nanotip. To gain a more comprehensive understanding, additional optical experiments and electromagnetic simulations are conducted. A direct irradiation experiment using a  $532 \text{ nm}$  laser ( $5.1 \text{ mW}$ ), focused by a  $50\times$  objective, shows no temperature rise in the substrate, attributed to

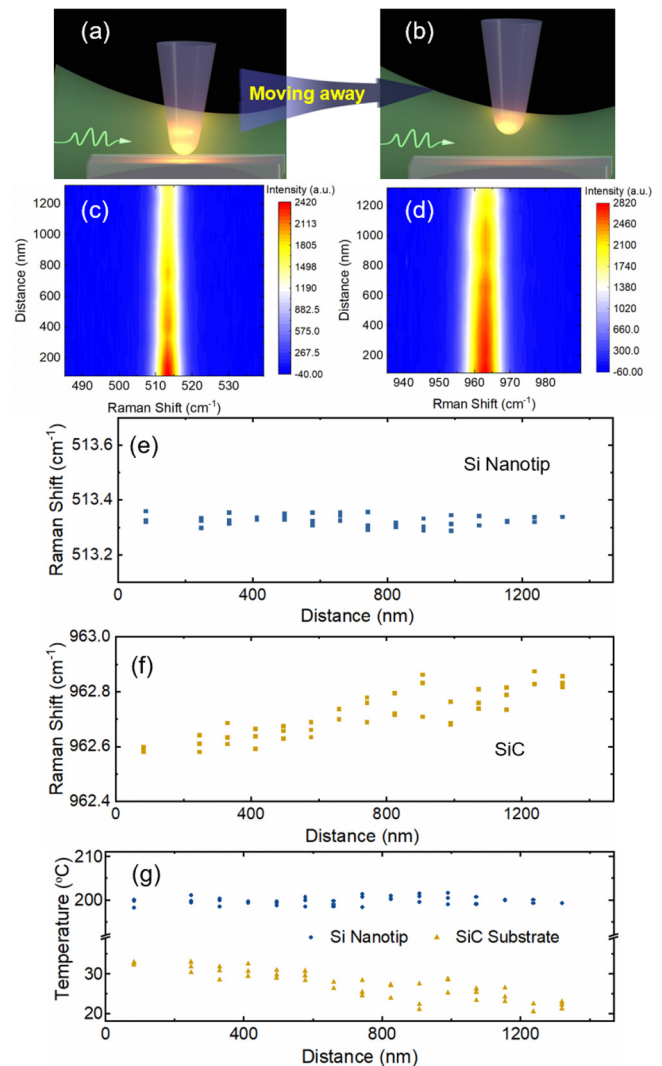


**FIG. 2.** The Si nanotip moving away from SiC substrate from (a) near contact mode to (b) a distance of about  $1320.0 \text{ nm}$ . Raman scattering intensities of (c) Si nanotip and (d) SiC substrate at various clearances. Raman shifts of (e) Si nanotip and (f) SiC substrate as a function of gap size. (g) Temperatures of Si nanotip and SiC substrate at different gap sizes.

the low absorptivity of SiC at  $532 \text{ nm}$  wavelength.<sup>24</sup> Furthermore, finite element simulations ([supplementary material](#) Note 2) based on three-dimensional Maxwell governing equations demonstrated no significant electromagnetic field enhancement in the substrate, even at the minimal gap size of  $82.5 \text{ nm}$  under experimental conditions (see [Fig. S2](#)). Therefore, the temperature elevation detected in the substrate during experiments is primarily due to heat transfer between the tip and the substrate, dependent on their respective temperatures and proximity. This high temperature facilitates heat transfer between the nanotip and the substrate, thereby underscoring a significant enhancement in heat transfer at nanoscale distances. The observation is thought to be linked to intensified air conduction and radiation as validated by previous theoretical studies.<sup>8,25</sup> Our research introduces a novel non-contact

technique for directly measuring temperatures on each side. This approach, compared to thermal resistivity-based methods, which involve inaccurate thermal resistance between the hot/cold surface and the measuring spot, significantly reduces measurement uncertainty.

Given the non-flat nature of the nanotip apex, the substrate surface directly beneath the nanotip experiences the highest level of heating. Due to the nanoscale size of the tip apex, with a radius of approximately 10 nm, it is inferred that thermal transport in the heated SiC substrate area is limited by ballistic heat transfer, leading to a smaller thermal conductivity.<sup>26,27</sup> This limitation results in a temperature change as the nanotip moves away. Previous study has shown that the thermal conductivity of Si and GaN can be reduced to about 10% of their bulk values when the heater size is less than 50 and 100 nm, respectively.<sup>26</sup> Note that the total heating radius could be larger than the tip apex since it accounts for all the heat transfer phenomena happening at the vicinity of the tip, which is very complicated.<sup>28</sup> In addition, the probe can suffer from thermal drift and small variations that could affect the accuracy of that distance. In our experiments, the drift of the nanotip attributable to thermal and vibrational fluctuations is within several nanometers,<sup>29,30</sup> which does not show a significant effect on the control of the gap size. It is also the reason we choose a minimum gap size of 82.5 nm, as controlling the gap size at much smaller distances proves challenging. To minimize the effect, we maintain the probe in a steady state during the measurement. Furthermore, the probe's temperature remains nearly constant during the measurement, significantly reducing thermal drift.

The heat transfer mechanisms associated with the nanotip are depicted in Figs. 3(a)–3(c). These involve heat absorption by the nanotip ( $Q_{\text{laser}}$ ), heat dissipation to the upper part ( $Q_{\text{up}}$ ) through thermal conduction to the cantilever and thermal convection to the surroundings, and heat dissipation to the substrate ( $Q_{\text{gap}}$ ) through both radiation and air conduction. As the nanotip moves away, its temperature

remains relatively stable despite these intricate surrounding conditions, leading to a diminished heating effect on the substrate. To deepen our understanding of the thermal transport process, theoretical calculations are performed focusing on air conduction and radiation between the nanotip and substrate.

Given the sub-wavelength scale distance between the tip and substrate, heat transfer across the air gap is critically affected, especially when the clearance nears the mean free path of ambient air, resulting in a transition regime, and ballistic effect on thermal conductivity is considered (see [supplementary material](#) Note 3). We discretize the air gap region into concentric cylindrical sections<sup>7</sup> with different gap distance  $D_i$ , as depicted in Fig. 3(c). For gap clearance  $\leq 400$  nm, the heat conduction is treated as being in a transition regime. The effective thermal conductivity for each layer, based on its local clearance, is applied to calculate air conduction discretely. The air thermal conductivity is assumed to adhere to its bulk value for gap distance beyond 400 nm. Considering the minimal change in average air temperature during the experiment (less than 6 °C) and the small variation in air thermal conductivity (<1.1%),<sup>31</sup> the heat transfer enhancement due to temperature increase in the air is neglected. Our computational analysis demonstrates an air conduction of  $1.45 \times 10^{-6}$  W at a gap distance of 82.5 nm and  $1.38 \times 10^{-7}$  W at 1320.0 nm, as shown in Fig. 3(d). A significant reduction, by a factor of 9.51, in air conduction is observed as the tip moves away from the substrate, showing a substantial enhancement in air conduction as the gap distance decreases.

In addition, near-field thermal radiation becomes critical at sub-wavelength scale gap distances.<sup>32,33</sup> To analyze this phenomenon, we calculate the radiation heat transfer intensity at each angular frequency and integrate these intensities over an angular frequency range from 0 to infinity to obtain the radiation flux, where the wavelength, temperature, and dielectric function of the materials involved are carefully

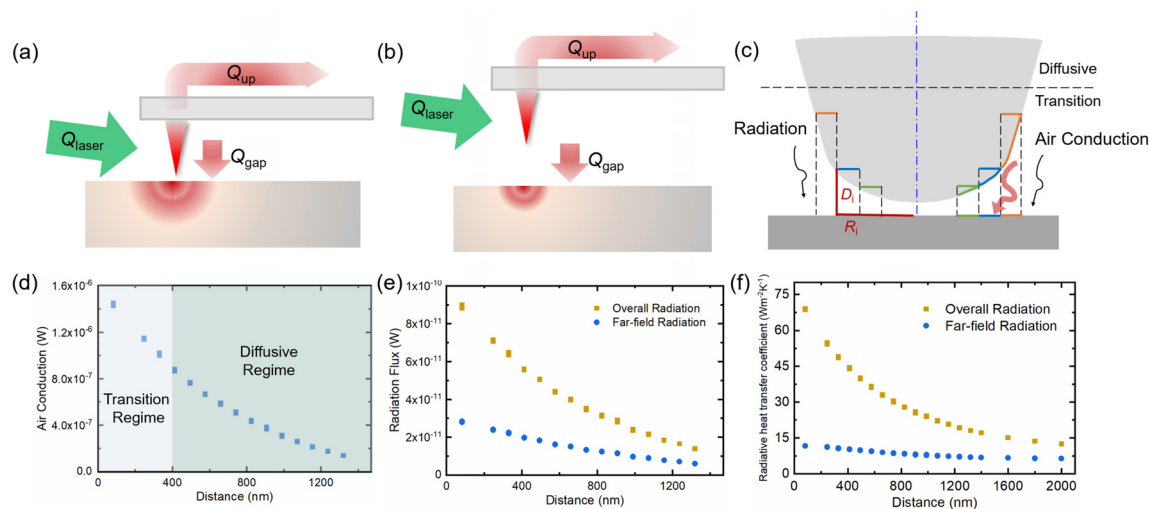


**FIG. 3.** Heat transfer processes of the nanotip–substrate system at (a) near contact mode and at a (b) significant distance. Nanotip absorbs heat due to laser irradiation ( $Q_{\text{laser}}$ ). This heat is subsequently transferred to the upper part of the tip and the surroundings through heat conduction and convection ( $Q_{\text{up}}$ ), and transferred to the substrate ( $Q_{\text{gap}}$ ) beneath the tip via air conduction and radiation. (c) Schematic showing the decomposition of tip–substrate air gap used for air conduction and radiation calculation. (d) Air conduction, (e) radiation flux, and (f) radiative heat transfer coefficient vs tip–substrate gap size.



considered. The computational analysis of theoretical radiative flux is conducted based on fluctuational electrodynamics, as detailed in [supplementary material](#) Note 3. Utilizing the Derjaguin approximation<sup>34</sup> and employing a discretization method as similar to that used in the air conduction calculations, the local radiative fluxes between two parallel plates at varying distances are calculated<sup>34,35</sup> and integrated to determine the overall radiative flux.

Figure 3(e) displays the theoretical radiative heat flux, which shows a monotonic decrease as the nanotip moves away from the substrate, diminishing from  $8.8 \times 10^{-10}$  to  $9.6 \times 10^{-11}$  W (a reduction by 9.17 times) as the gap distance increases from 82.5 to 1320.0 nm. Similar with the trends observed in air conduction, radiation experiences a significant enhancement as the gap distance goes down to tens of nanometers. Moreover, we calculate the theoretical overall and far-field radiation heat transfer coefficients between Si and SiC plates at various gap size as illustrated in Fig. 3(f). Specifically, at a gap distance of 82.5 nm and temperatures corresponding to those observed in the experiments, the computed values for the theoretical overall and far-field radiation heat transfer coefficients are 69.0 and 11.7 W/(m<sup>2</sup>K), respectively, underscoring the notable impact of evanescent waves on radiation at the nanoscale. For the nanotip–substrate system, the enhancement in radiation is less pronounced than the radiation heat transfer coefficient, due to a significant portion of the nanotip being distant from the substrate. Therefore, in addition to the near-field effect, factors such as the increased heat exchange area and angle factor within the nanotip–substrate system play vital roles in the enhancement of radiative flux as the gap distance decreases. The radiative heat flux is three orders of magnitude lower than the air conduction heat flux, indicating the dominant role of air conduction in the heat transfer between the nanotip and substrate, thereby rendering radiation relatively negligible.

In summary, a Raman-based technique is developed to characterize enhanced heat transfer across a nanogap. This method overcomes the measurement uncertainties commonly accompanied by conventional methods and demonstrates its applicability by successfully characterizing the significant enhancement in heat transfer between a Si nanotip and a SiC substrate as their gap distance decreases. Utilizing the relationship between the Raman spectrum and temperature, our method enables direct temperature measurement of both the nanotip and the substrate. We report a distinct decrease in substrate temperature as the nanotip moves away from it. And computational results indicate that air conduction and radiation flux decrease by approximately nine times as the gap distance increases from approximately 82.5 nm to about 1.32  $\mu$ m. Our method constitutes a step toward realizing heat transfer characterization at sub-wavelength distance between nanostructured surfaces for thermal management at the nanoscale.

See the [supplementary material](#) for details on Raman thermal measurement calibration, electromagnetic simulation of the tip–substrate system, and theoretical calculation methods.

This study was financially supported by the National Key Research and Development Program of China (No. SQ2023YFE0102578) and the National Natural Science Foundation of China (No. 52076156). The authors appreciate the support from the Supercomputing Center and Large-scale Instrument and Equipment Sharing Foundation of Wuhan University.

## AUTHOR DECLARATIONS

### Conflict of Interest

The authors have no conflicts to disclose.

### Author Contributions

**Xiaona Huang:** Data curation (equal); Formal analysis (equal); Visualization (equal); Writing – original draft (equal). **Qiangsheng Sun:** Data curation (equal); Formal analysis (equal). **Shen Xu:** Formal analysis (equal); Writing – review & editing (equal). **Yanan Yue:** Conceptualization (equal); Formal analysis (equal); Funding acquisition (equal); Supervision (equal); Writing – review & editing (equal). **Xinwei Wang:** Conceptualization (equal); Writing – review & editing (equal). **Yimin Xuan:** Conceptualization (equal); Writing – review & editing (equal).

### DATA AVAILABILITY

The data that support the findings of this study are available from the corresponding author upon reasonable request.

### REFERENCES

- L. Zhu, A. Fiorino, D. Thompson, R. Mittapally, E. Meyhofer, and P. Reddy, “Near-field photonic cooling through control of the chemical potential of photons,” *Nature* **566**(7743), 239–244 (2019).
- C. Lucchesi, D. Cakiroglu, J.-P. Perez, T. Taliere, E. Tournié, P.-O. Chapuis, and R. Vaillon, “Near-field thermophotovoltaic conversion with high electrical power density and cell efficiency above 14%,” *Nano Lett.* **21**(11), 4524–4529 (2021).
- E. Albisetti, D. Petti, M. Pancaldi, M. Madami, S. Tacchi, J. Curtis, W. King, A. Papp, G. Csaba, and W. Porod, “Nanopatterning reconfigurable magnetic landscapes via thermally assisted scanning probe lithography,” *Nat. Nanotechnol.* **11**(6), 545–551 (2016).
- S. Lefèvre, S. Volz, and P.-O. Chapuis, “Nanoscale heat transfer at contact between a hot tip and a substrate,” *Int. J. Heat Mass Transfer* **49**(1–2), 251–258 (2006).
- S. Zhang, Y. Dang, X. Li, Y. Li, Y. Jin, P. Choudhury, J. Xu, and Y. Ma, “Transient measurement of near-field thermal radiation between macroscopic objects,” *Nanoscale* **16**(3), 1167–1175 (2024).
- X. Liu and Z. Zhang, “Near-field thermal radiation between metasurfaces,” *ACS Photonics* **2**(9), 1320–1326 (2015).
- Y. Zhang, W. Zhu, and T. Borca-Tasciuc, “Thermal conductivity measurements of thin films by non-contact scanning thermal microscopy under ambient conditions,” *Nanoscale Adv.* **3**(3), 692–702 (2021).
- Y. Zhang, W. Zhu, L. Han, and T. Borca-Tasciuc, “Quantitative temperature distribution measurements by non-contact scanning thermal microscopy using Wollaston probes under ambient conditions,” *Rev. Sci. Instrum.* **91**(1), 014901 (2020).
- K. Kim, B. Song, V. Fernandez-Hurtado, W. Lee, W. Jeong, L. Cui, D. Thompson, J. Feist, M. T. Reid, F. J. Garcia-Vidal, J. C. Cuevas, E. Meyhofer, and P. Reddy, “Radiative heat transfer in the extreme near field,” *Nature* **528**(7582), 387–391 (2015).
- H. Salihoglu, W. Nam, L. Traverso, M. Segovia, P. K. Venuthurumilli, W. Liu, Y. Wei, W. Li, and X. Xu, “Near-field thermal radiation between two plates with sub-10 nm vacuum separation,” *Nano Lett.* **20**(8), 6091–6096 (2020).
- J. DeSutter, L. Tang, and M. Francoeur, “A near-field radiative heat transfer device,” *Nat. Nanotechnol.* **14**(8), 751–755 (2019).
- X. Luo, H. Salihoglu, Z. Wang, Z. Li, H. Kim, X. Liu, J. Li, B. Yu, S. Du, and S. Shen, “Observation of near-field thermal radiation between coplanar nanodevices with subwavelength dimensions,” *Nano Lett.* **24**(5), 1502–1509 (2024).
- X. Huang, Y. Wang, S. Deng, and Y. Yue, “Laser polarization associated periodic oscillation of thermal response in silicon nanotip,” *Int. J. Heat Mass Transfer* **209**, 124124 (2023).
- C. Li, S. Xu, Y. Yue, B. Yang, and X. Wang, “Thermal characterization of carbon nanotube fiber by time-domain differential Raman,” *Carbon* **103**, 101–108 (2016).

- <sup>15</sup>A. Fan, Y. Li, W. Ma, H. Wang, and X. Zhang, "Opto-electric flash Raman method for in situ measuring temperature variation of power device with a high temporal resolution," *Appl. Therm. Eng.* **217**, 119190 (2022).
- <sup>16</sup>S. Chen, A. L. Moore, W. Cai, J. W. Suk, J. An, C. Mishra, C. Amos, C. W. Magnuson, J. Kang, and L. Shi, "Raman measurements of thermal transport in suspended monolayer graphene of variable sizes in vacuum and gaseous environments," *ACS Nano* **5**(1), 321–328 (2011).
- <sup>17</sup>A. A. Balandin, S. Ghosh, W. Bao, I. Calizo, D. Teweldebrhan, F. Miao, and C. N. Lau, "Superior thermal conductivity of single-layer graphene," *Nano Lett.* **8**(3), 902–907 (2008).
- <sup>18</sup>P. Sokalski, Z. Han, G. C. Fleming, B. Smith, S. E. Sullivan, R. Huang, X. Ruan, and L. Shi, "Effects of hot phonons and thermal stress in micro-Raman spectra of molybdenum disulfide," *Appl. Phys. Lett.* **121**(18), 182202 (2022).
- <sup>19</sup>D. Huang, Q. Sun, Z. Liu, S. Xu, R. Yang, and Y. Yue, "Ballistic thermal transport at sub-10 nm laser-induced hot spots in GaN crystal," *Adv. Sci.* **10**, e2204777 (2022).
- <sup>20</sup>R. Wang, S. Xu, Y. Yue, and X. Wang, "Thermal behavior of materials in laser-assisted extreme manufacturing: Raman-based novel characterization," *Int. J. Extreme Manuf.* **2**(3), 032004 (2020).
- <sup>21</sup>S. Hamian, J. Yun, I. Park, and K. Park, "Quantitative probing of tip-induced local cooling with a resistive nanoheater/thermometer," *Appl. Phys. Lett.* **109**(25), 253114 (2016).
- <sup>22</sup>M. Bauer, A. M. Gigler, A. J. Huber, R. Hillenbrand, and R. W. Stark, "Temperature-depending Raman line-shift of silicon carbide," *J. Raman Spectrosc.* **40**(12), 1867–1874 (2009).
- <sup>23</sup>S. Deng, S. Xu, J. Gao, H. Wu, J. She, and Y. Yue, "Picosecond-resolved Raman response of a Si nanotip for probing temperature and thermal stress in the confined regime under laser heating," *J. Phys. Chem. C* **126**, 1922 (2022).
- <sup>24</sup>R. Ahuja, A. Ferreira da Silva, C. Persson, J. Osorio-Guillen, I. Pepe, K. Järrendahl, O. Lindquist, N. Edwards, Q. Wahab, and B. Johansson, "Optical properties of 4H-SiC," *J. Appl. Phys.* **91**(4), 2099–2103 (2002).
- <sup>25</sup>A. Fiorino, L. Zhu, D. Thompson, R. Mittapally, P. Reddy, and E. Meyhofer, "Nanogap near-field thermophotovoltaics," *Nat. Nanotechnol.* **13**(9), 806–811 (2018).
- <sup>26</sup>Y. Hu, L. Zeng, A. J. Minnich, M. S. Dresselhaus, and G. Chen, "Spectral mapping of thermal conductivity through nanoscale ballistic transport," *Nat. Nanotechnol.* **10**(8), 701–706 (2015).
- <sup>27</sup>G. Mahan and F. Claro, "Nonlocal theory of thermal conductivity," *Phys. Rev. B* **38**(3), 1963 (1988).
- <sup>28</sup>Y. Zhang, W. Zhu, F. Hui, M. Lanza, T. Borca-Tasciuc, and M. Muñoz Rojo, "A review on principles and applications of scanning thermal microscopy (SThM)," *Adv. Funct. Mater.* **30**(18), 1900892 (2020).
- <sup>29</sup>Y. Okada and Y. Tokumaru, "Precise determination of lattice parameter and thermal expansion coefficient of silicon between 300 and 1500 K," *J. Appl. Phys.* **56**(2), 314–320 (1984).
- <sup>30</sup>R. Kato, T. Moriyama, T. Umakoshi, T.-A. Yano, and P. Verma, "Ultraprecise tip-enhanced hyperspectral optical nanoimaging for defect analysis of large-sized WS<sub>2</sub> layers," *Sci. Adv.* **8**(28), eabo4021 (2022).
- <sup>31</sup>F. Ochs, W. Heidemann, and H. Müller-Steinhagen, "Effective thermal conductivity of moistened insulation materials as a function of temperature," *Int. J. Heat Mass Transfer* **51**(3–4), 539–552 (2008).
- <sup>32</sup>J.-P. Mulet, K. Joulain, R. Carminati, and J.-J. Greffet, "Nanoscale radiative heat transfer between a small particle and a plane surface," *Appl. Phys. Lett.* **78**(19), 2931–2933 (2001).
- <sup>33</sup>B. Song, Y. Ganjeh, S. Sadat, D. Thompson, A. Fiorino, V. Fernandez-Hurtado, J. Feist, F. J. Garcia-Vidal, J. C. Cuevas, P. Reddy, and E. Meyhofer, "Enhancement of near-field radiative heat transfer using polar dielectric thin films," *Nat. Nanotechnol.* **10**(3), 253–258 (2015).
- <sup>34</sup>D. Polder and M. Van Hove, "Theory of radiative heat transfer between closely spaced bodies," *Phys. Rev. B* **4**(10), 3303 (1971).
- <sup>35</sup>T. Tokunaga, A. Jarzembki, T. Shiga, K. Park, and M. Francoeur, "Extreme near-field heat transfer between gold surfaces," *Phys. Rev. B* **104**(12), 125404 (2021).